Received 26 February 2007
Revised 25 May 2007
Accepted 25 May 2007

Numerical analysis and experimental validation of the free surface flow and heat transfer in electrical transformers moulding processes

Zbigniew Buliński and Andrzej J. Nowak
Faculty of Institute of Thermal Technology, Silesian University of Technology, Gliwice, Poland

Abstract

Purpose – The purpose of this paper is to present a numerical and mathematical model of a moulding process of a dry electrical transformer. Moreover, the calculated results are reported and compared with experimental measurements.

Design/methodology/approach – An experimental rig, for carrying out and monitoring a moulding process, has been designed and built. Two experiments were preformed. First was an isothermal experiment in which an analog liquid was used. The second experiment was a non-isothermal one in which an epoxy resin was used. For the rig geometry, the numerical mesh, with the use of the commercial code Gambit, was built. All necessary physical properties, including viscosity, surface tension and contact angle of fluids used in the experiments were measured.

Findings – The Euler approach for modelling multiphase flow with a free surface is addressed in the presented work. Comparison of the computational results with measurements on the designed experimental rig revealed good agreement. Comparison was carried out through measurements of free surface characteristic features captured with a digital camera and through temperature measurements for the nonisothermal case. Richardson extrapolation method was successfully applied to estimate the numerical discretisation error, proving that a grid independent solution was obtained.

Originality/value – This paper is useful for researchers and industrialists involved in the modelling of moulding processes, giving guidance on the available mathematical models appropriate for this kind of problem. Moreover, it provides valuable information as to how to perform validation and verification procedures for such real-life processes.

Keywords Numerical analysis, Simulation, Flow, Heat transfer, Mouldability

Paper type Research paper

This research has been financed by the Polish Ministry of Science and Higher Education within Grant N512 022 31/2577. This assistance is gratefully acknowledged herewith. This research would not have been possible without the help of the ABB Corporate Research Centre and this is gratefully acknowledged also. The authors would also like to express their gratitude to the Department of Chemical and Process Apparatus Construction of the Silesian University of Technology and the Department of Paints and Plastics in the Institute of Plastics Processing in Gliwice for their help in the measurement of the physical properties of analog liquid and epoxy resin.

International Journal of Numerical Methods for Heat & Fluid Flow
Vol. 18 No. 3/4, 2008
pp. 356-377

0961-5539
DOI 10.1108/09615530810853628

1. Introduction

During the last 30 years or so, an incredible development and a dramatic cost decrease in computers has caused them becoming one of the most important tools in the work of a modern engineer in the modelling fluid and heat flows. Computational fluid dynamic (CFD) techniques are efficiently used in conceptual studies of new designs, detailed product development, troubleshooting or redesign, optimisation and control of many industrial processes, etc. Broad use of CFD in industrial applications has resulted in more complicated problems being solved. However, each CFD code and simulation needs to be inspected if the obtained results are reliable. This objective can be accomplished by means of a credibility analysis (or validation & verification – V&V analysis) of the numerical model (Babuska and Oden, 2004; Banaszek, 2005).

Credibility analysis (V&V analysis) consists of two fundamental aspects: verification and validation. The main objective of simulation validation is ensuring if the physical process is properly described by the governing mathematical equations, i.e. whether the correct equations are being solved. Technically, validation is accomplished by comparison of the calculated results with those obtained in the analogous experiment. On the other hand, verification addresses the correctness of the solution of the model equations. The verification procedure consists of two steps, first is a code verification which addresses the coding errors in the simulation software. In the second step, the solution verification occurs to quantify the numerical errors which appear during the solution procedure. In case of a very sophisticated industrial application usually there are not exist appropriate benchmark solutions to verify the solution. In such a case, exact solution extrapolation may be used based on a grid refinement study. Detailed description of these methods can be found in Roy (2005).

Electrical transformers are very important parts of many industrial power supply systems. Their proper and reliable operation is crucial for the correct course of many industrial processes. Only functional and reliable insulation ensures proper operation of these electrical devices. This is particularly important in the case of devices operating in rigorous ambient conditions. Usually, transformers, which work in such conditions, are built as the dry-type ones. All electrical circuits of such a device are enclosed in tight casings made of epoxy resin, whose main function is the electrical insulation of the device. It should also separate internal parts of the transformer from the influence of external conditions. Moreover, it must ensure that it carries away heat produced inside the transformer. To assure the proper fulfilment of these tasks, the transformer epoxy casing must be free of any internal failures, such as air voids or material discontinuities.

Most of dry-type electrical transformers are produced in so-called Vacuum Casting Technology (often under sub-atmospheric pressure). In this technology, the internal elements of the transformer are placed in a mould which is then filled with an epoxy resin composition. After the introductory curing in the mould, the casting is further cured outside the mould by heating it in a tunnel furnace. Crucial for a proper process proceeding, and hence for product quality is the mould filling stage during which problems such as incomplete filling, air voids and bubbles may arise. Very long product development and high costs of a single element is of great importance to be able to predict and overcome any potential troubles. Such possibilities are given by CFD simulations (Sekuła *et al.*, 2002). Since, this is a very advanced application of the CFD tool it needs extensive verification and validation.

In this work, the approach to such a V&V analysis is presented. This work focuses on the verification and validation of the mathematical model of tracing the phase interface. Based on information from a real-life epoxy casting technology and construction of voltage transformers, the model of the casting stand is designed and built up. This stand allows us to carry out and record cold and hot transformer casting processes under atmospheric conditions. Two kinds of experiments are carried out, namely isothermal and non-isothermal. In the first one an analog fluid is used instead epoxy resin, and no heat transfer is considered. In the second experiment, epoxy resin is used and the internal parts of the transformer are heated up. For such defined processes, the mathematical and numerical models, with the use of the commercial CFD code Fluent, are created. Results from the numerical calculations are compared with those obtained from the experiment.

2. Experimental validation

Instrument electrical transformers are commonly used in measuring and controlling systems of power plants. They separate measuring instruments from primary circuits, and prevent any damage due to short-circuit currents. They are also used to extend the measuring range of standard devices. Based on the dimensions of the common voltage transformer UMZ-24 produced in ABB's plant in Poland (Figure 1), the experimental stand for the casting of such a transformer is designed and built. The main three parts of the experimental stand are the same in both isothermal and non-isothermal experiments (Figures 2 and 3):

(1) glass tank (casting mould);

(2) inner transformer element; and

(3) resin feeding system.

Numerical analysis requires the exact specification of the geometry, boundary and initial conditions, and physical properties of the materials which take part in the process. In the case of real-life industrial processes, exact specification of these model parameters may be extremely difficult or even impossible. Therefore, during the design stage of the experimental stand, a few simplifying assumptions concerning the geometry,

Figure 1.
UMZ-24 medium voltage instrument transformer

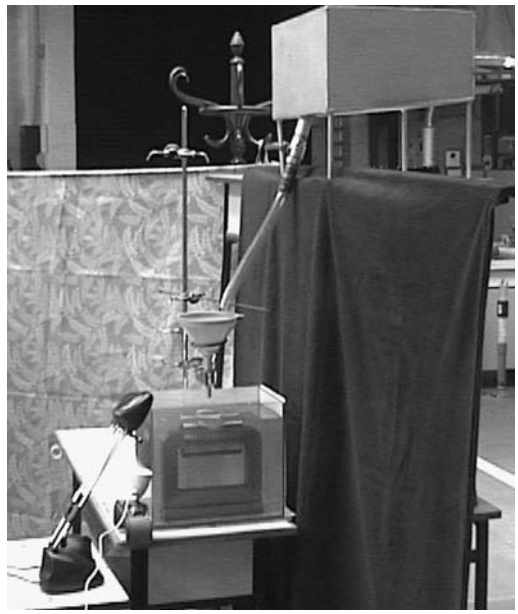

Figure 2.
Experimental stand for the non-isothermal transformer moulding process experiment

construction and casting process were made. These simplifications are insignificant and do not cause a large distortion compared to the original problem. However, they allow avoiding any additional simplification at the mathematical modelling stage. The original shape of the transformer mould has been simplified to a rectangular prism and this considerably facilitates the numerical mesh generation. The mould in the experiment should allow the tracing and filming the position and shape of the liquid free surface. It must also be durable and easy to clean. That is the reason why the mould has been made of glass. The main internal parts of the voltage transformer are: core made of steel sheets, primary and secondary coils wound concentrically around one arm of the core, connectors which establish connections between windings and phase terminals. Figure 4 shows an example of an original transformer winding and its counterpart used in the experiments. As it can be seen, its geometry has been simplified and this has resulted in a considerably simplified mesh generation. Moreover, the core and the coil have been made of one solid piece of steel whose properties are well defined. The connectors are represented by the solid rectangular prism of steel with dimensions: length 250 mm, width 90 mm and height 20 mm. The feeding system was designed as a gravitational one (Figures 2 and 3), where the driving force is the difference between the free surface of the liquid in the main tank and the level of the inlet to the mould. It consisted of two main elements: the feeding tank and the funnel. The feeding tank had the following dimensions: length 400 mm, width 400 mm and height (the smallest one) 200 mm. It was equipped with a one inch stub pipe with a ball valve placed in its bottom. The stub pipe was connected with a 0.5 m long rubber hose of the same diameter. The bottom of the tank is inclined towards the stub pipe to empty the tank relatively easy. The ball valve allowed the control of the liquid mass flow rate. Simplified calculations were carried out to match the appropriate dimensions of the funnel to meet

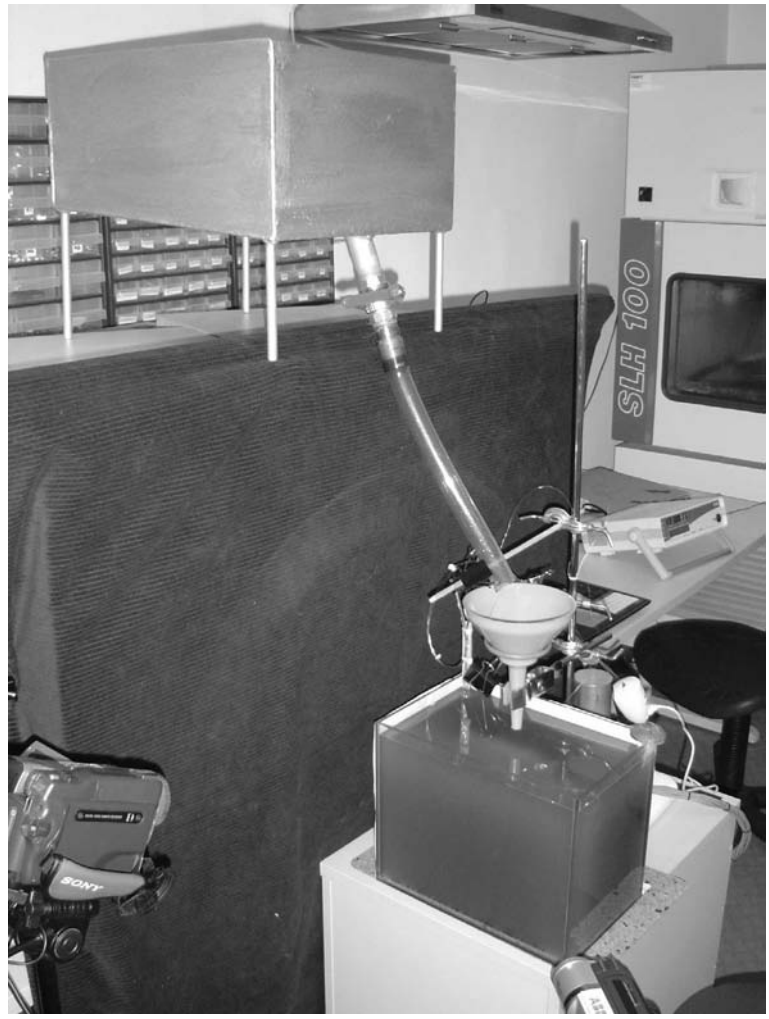

Figure 3.
Experimental stand for the isothermal transformer moulding process experiment

this constraint (Buliński, 2004). Complete experimental stands for both experiments are shown in Figures 2 and 3.

On the surfaces of some of the internal elements, grids have been plotted which would allow us to validate the free surface mapping (Figures 5 and 6). Vertical lines on the coil surface were plotted every 1 cm to measure the width of the flowing liquid at the top of the coil, while horizontal lines, which were made every 20° on the upper half and every 10° on the lower half of the coil, allowed us to capture the separation point of the liquid from the coil surface. Rectangular grids made on the bottom arm of the core had lines drawn every 1 cm, and this made it possible for us to show the point at which liquid dropped on the core and to trace the movement of the contact line on the core surface. Grids with the same density were made on the part of the mould bottom

Figure 4.
Simplified experimental transformer core with a solid coil and its original counterpart

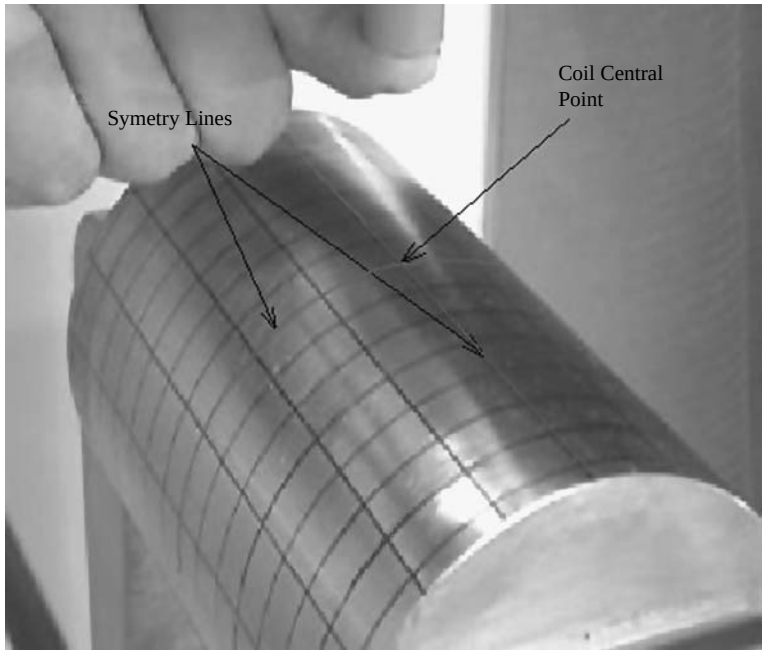

Figure 5.
Grid plotted on the surfaces of the transformer coil

(on the plexiglass plate). The red lines indicate the symmetry planes of the model. This allowed the tracing movements of the contact line across the plate (Buliński, 2004).

Three digital cameras were used to film both experiments (Figure 7). They were located appropriately to assure the best capture of the shape of the flowing free surface. Of major interest were the top of the coil and the bottom arm of the coil, where very interesting shapes of the phase interface were observed. The employed cameras

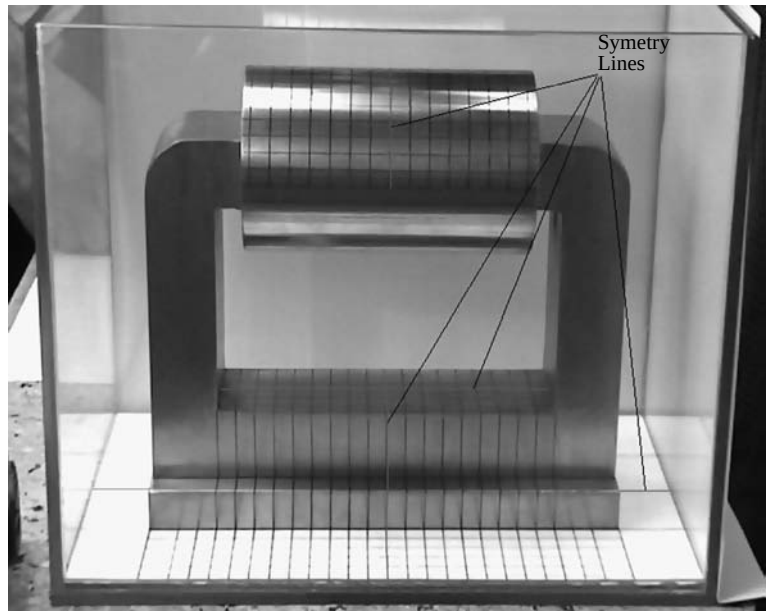

Figure 6.
Grids plotted on the surfaces of the transformer internal parts and the bottom of the mould

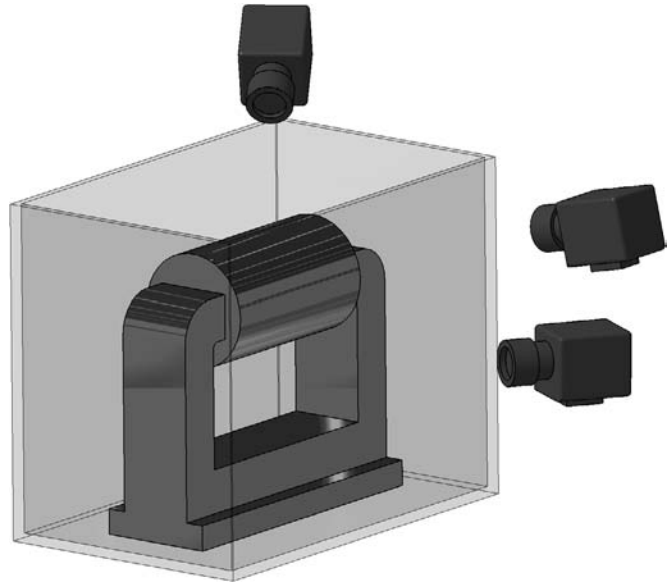

Figure 7.
Digital camera set up during the experiment

captured 25 frames per second with a resolution up to 720 × 576. Additional spot-lighting and set of simple screens were employed. Moreover, two mould walls were covered with white sheets of paper. This ensured the appropriate illumination of the position and eliminated any light reflections from highly polished surfaces of the internal elements and glass walls of the mould.

In the cold experiment 131 of analog liquid were used to fill the mould in which internal elements were placed previously. The funnel had a height 190 mm and outlet diameter 11 mm and this resulted in a filling time of 117.5 s. In this experiment, all elements of the stand, i.e. mould, internal elements, feeding system as well as the liquid itself were at the ambient temperature. Therefore, in the mathematical description of the process the energy equation was neglected. The hot experiment was carried out with two-component epoxy composition by Bakelite AG as a filling medium. This resin is characterised by a very long curing time, in ambient conditions complete curing lasted up to about one month. This should be compared with the filling time which in this case was equal to 300 s. Those effects related to the curing of the composition, such as the influence on the physical properties or heat released during the reaction could be neglected in the mathematical model. Temperature of the epoxy composition during the experiment was measured with a coat thermocouple placed in the funnel, it was at 293.45 K. Six more thermocouples were placed inside the mould near its walls (Figure 8). The mould initially had an ambient temperature 297.1 K. Before whole experiment was started, internal elements of the transformer were heated up to 393 K. Measurement data were collected by the data logger connected to the PC computer. In general, both experiments proceeded in the same manner. After filling the tank with the liquid (washing up liquid/epoxy resin) and setting the internal elements and thermocouples (in the case of the non-isothermal experiment) inside

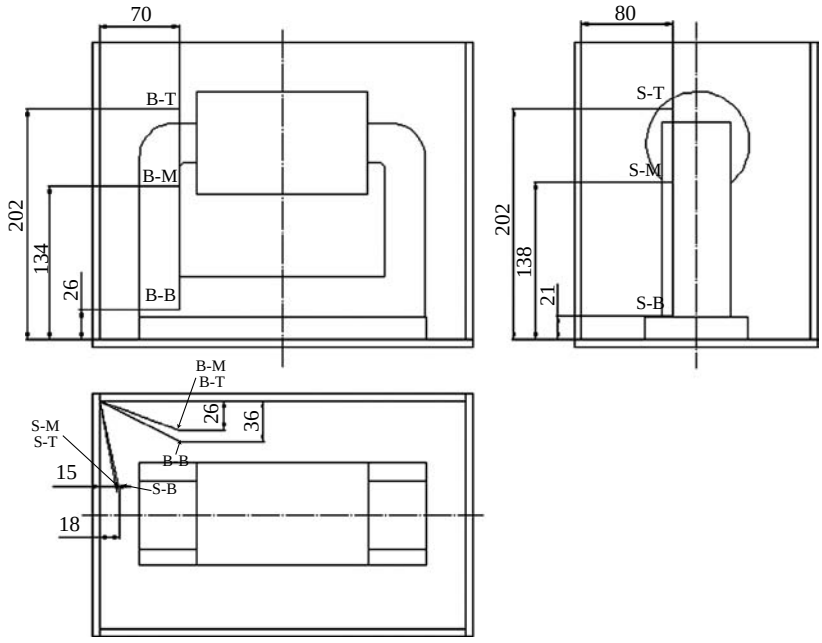

Notes: S-B - side-bottom; S-M - side-middle; S-T - side-top; B-B - back-bottom; B-M - back-middle; B-T - back-top

Figure 8.
Location of thermocouples placed inside the casting mould

the mould, the funnel outlet was plugged and the funnel was filled to the reference level with the liquid. Then simultaneously the funnel outlet was unplugged and the tank valve was opened to keep the level of the liquid constant. While the filling process proceeded, the ball valve was being gradually opened to keep a constant level of the liquid in the funnel as the surface of liquid in the feeding tank was dropping. This allowed us to maintaining the volumetric flow rate of the liquid during casting to be almost constant (Buliński, 2004).

3. Mathematical and numerical model of the free surface flow

The two main approaches to the modelling of multiphase flows are Eulerian or Lagrangian. In the first approach different phases are treated as interpenetrating continuum fluids, and this description may cover a very large set of problems. In this approach, a few methods may be distinguished. A single set of flow equations might be solved for all the phases, properties are calculated as weighted average values and some models are applied to account for the interfacial forces or each phrase possess own set of flow equations this is the so-called multifluid formulation. However, all these formulations have in common that the calculations are carried out on a stationary grid. The different phases are distinguished by a marker function which specifies the volumetric fraction of a given phase in a cell. In the Lagrangian approach, only the primary phase may be considered as a continuum, and all other phases are modelled as a set of particles which move within and interact with the continuum phase. This method is restricted mainly to dispersed flows. For free surface flows, in general the Eulerian formulation is preferred. However, there are examples of utilisation of the Lattice Boltzman method for these kind of problems (Mingming and Browne, 2005).

In the case of Eulerian modelling of free surface flows one must know the position of the phase interface since a rapid change in the physical properties take place across it. Therefore, it is very important to accurately capture its location and shape. A number of scientists are working on this nontrivial task, and a general review of the interface capturing methods may be found in Mingming and Browne (2005) and Tryggvason *et al.* (2001). The two most widely used methods are Marker and Cell (Harlow and Welsh, 1965) and volume of fluid (VOF) method (Hirt and Nichols, 1981). Since, it is less computationally expensive, the second approach is most widely used in commercial CFD codes and it was also used in this work.

3.1 Governing equations

The VOF formulation, proposed by Hirt and Nichols (1981) is designed for two or more phases (fluids) which do not interpenetrate each other. For each phase a new variable α_i is defined: the volume fraction of that specific phase in a computational cell. It describes simply to what extend the given computational cell is filled with that phase. There are three possible situations for an arbitrary i-th phase: $\alpha_i = 0$ there is no i-th phase in the cell, $\alpha_i = 1$ the cell is completely filled with i-th phase and $0 < \alpha_i < 1$ if the cell contains the phases interface. To calculate the phase volume fractions in all computational cells, for each secondary phase a transport equation of volume fraction is introduced. The volume fraction of a primary phase meets complements volumetric fraction of all phases to one. The flow of a

multiphase mixture is described by one set of volume-averaged conservation equations common for all phases. In the case of a two phase system only one additional transport equation is solved.

3.1.1 Phase transport equation. In the calculated cases, the analog liquid or resin were treated as secondary phases. Hence, their flow and position of the free surface was described by the volume fraction transport equation:

$$\frac{1}{\varrho_l}\left[\frac{\partial(\alpha_l\varrho_l)}{\partial t}+\nabla\cdot(\alpha_l\varrho_l w)\right]=0 \tag{1}$$

where the index l stands for analog liquid in the isothermal case and for epoxy resin in the non-isothermal case, ϱ_l is the density of the l-th phase, w is the velocity of the mixture. The volume fraction of air, which was treated in both cases as a primary phase, was calculated using the formula:

$$\alpha_a=1-\alpha_l \tag{2}$$

where α_a is the air volume fraction in a cell.

3.1.2 Flow equations. Both phases share the same velocity w and pressure p fields so a single set of flow equations is solved throughout the whole domain:

- Mass conservation equation:

$$\frac{\partial\varrho}{\partial t}+\nabla\cdot(\varrho w)=0 \tag{3}$$

- Momentum conservation equation for incompressible flows:

$$\frac{\partial(\varrho w)}{\partial t}+\nabla\cdot(\varrho ww)=-\nabla p+\nabla\cdot[\mu(\nabla w+\nabla w^{\mathrm{T}})]+\varrho g+F_\sigma \tag{4}$$

In the above equations, g is the gravitational acceleration, F_σ is the body force due to surface tension and it has a non zero value only in cells where the interface is located, ϱ is the volume average density of two-phase mixture:

$$\varrho=\alpha_l\varrho_l+\alpha_a\varrho_a \tag{5}$$

in the same manner the mean two-phase mixture viscosity is calculated:

$$\mu=\alpha_l\mu_l+\alpha_a\mu_a \tag{6}$$

3.1.3 Surface tension and wall adhesion. Surface tension was modelled using a continuum surface force model proposed by Brackbill *et al.* (1992). In this model, the surface tension is accounted for by the addition of an extra body force term F_σ in the momentum equation (4), in the computational cells through which the phase interface passes:

$$F_\sigma=2\sigma\frac{\kappa_l\varrho\nabla\alpha_l}{\varrho_l+\varrho_a} \tag{7}$$

where σ is the surface tension between the liquid and air, $\rangle$ is the average density calculated from equation (5), κ_l is the curvature of phases interface:

$$\kappa_l = \nabla \cdot \hat{\mathbf{n}}_l \tag{8}$$

where $\hat{\mathbf{n}}_l$ is the unit vector normal to the phase interface:

$$\hat{\mathbf{n}}_l = \frac{\nabla \alpha_l}{|\nabla \alpha_l|} \tag{9}$$

At the walls, with a known contact angle θ between the liquid phase and the wall, the unit normal vector is calculated in the following way:

$$\hat{\mathbf{n}}_l = \hat{\mathbf{n}}_w \cos\theta + \hat{\mathbf{t}}_w \sin\theta \tag{10}$$

where $\hat{\mathbf{n}}_w$ and $\hat{\mathbf{t}}_w$ are the unit vectors, normal and tangential to the wall, respectively. Then the combination of the unit normal vector calculated in this way (equation (10)) with the one calculated from equation (9) is used to estimate the interface curvature near the wall. This curvature is then used in the calculation of the body force resulting from the surface tension.

3.1.4 Energy equation. The assumption that the phases are in thermodynamic equilibrium results in a one temperature field shared by both phases and one energy equation:

$$\frac{\partial(\varrho h)}{\partial t} + \nabla \cdot w(\varrho h + p) = \nabla(\lambda_{\text{eff}} \nabla T) \tag{11}$$

where h is the specific enthalpy of two-phase mixture, calculated as a mass weighted average:

$$h = \frac{\alpha_l \varrho_l h_l + \alpha_a \varrho_a h_a}{\alpha_l \varrho_l + \alpha_a \varrho_a} \tag{12}$$

and λ_{eff} is the effective heat conduction coefficient, calculated as:

$$\lambda_{\text{eff}} = \alpha_a \lambda_a + \alpha_l \lambda_l \tag{13}$$

3.2 Physical properties

To be able to compare the computed result with the experimental results, the physical properties of the liquids used in the experiments should be known. Since, both used fluids were not well described in the available literature, their physical properties needed to be measured. In the non-isothermal experiment, epoxy resin which was used reacts very slowly in the experiment temperature range, therefore polimerisation reaction and its effects were not considered in the numerical simulation of this process. Preliminary differential scanning calorimeter (DSC) measurements reveal that this reaction considerably accelerates at temperature above 150°. However, the temperature in the experiment did not exceeded 120° and thereby it can be neglected in this analysis.

3.2.1 Analog liquid. In the case of the experiment without heat transfer, the density, dynamic viscosity coefficient and surface properties (surface tension and contact angles) were necessary for numerical calculations.

The density of analog liquid was measured using an aerometer, which utilizes the buoyancy effect in the measurements. The value measured in was 1,017 kg/m^3.

The dynamic viscosity coefficient was measured with utilisation of the Brookfield LVDV-III rotational rheometer. Rotational speeds from 0.1 up to 250 revolutions per minute were investigated, thus covering a very wide range of shear rates. Three liquid samples were measured, for each descending and ascending runs were preformed, to verify if the liquid revealed a tixotropic behaviour. Because of the lack of information regarding the rheology of the analog liquid, three mathematical models were assumed: Newtonian, Bingham and Ostwald-de Weale. In the Newtonian model, the shear stress τ is directly proportional to the shear rate $\dot{\gamma}$:

$$\tau = -\mu\dot{\gamma} \tag{14}$$

where the proportion constant is the dynamic viscosity coefficient μ, and its measured value was 2.53 kg/sm. In the case of the Bingham model:

$$\tau = \tau_0 + \mu_p\dot{\gamma} \tag{15}$$

and the yield stress τ_0 was 0.43 Pa and the plastic viscosity μ_p was 1.63 kg/sm. In the case of Ostwald-de Weale model:

$$\tau = m\dot{\gamma}^n \tag{16}$$

model parameters were equal: flow factor $n = 0.95$ and consistency coefficient $m = 1.7\,\mathrm{kg/s^{2-n}m}$. Numerical calculations were preformed for all three rheological models.

The surface tension was measured with the KRÜSS K-8600 tensiometer which utilises the Lacomte du Noüy ring method for the measurements. The sample temperature during measurements was 22°C and the measured value of surface tension was 0.03 N/m.

Contact angles between washing up liquid and appropriate steel, glass or plexiglass were determined using the sessile drop measuring method by taking a photograph of the drop placed on these materials, following values were obtained: contact angle liquid-steel 25° liquid-glass 30° and liquid-plexiglass 20°.

Further details on all the measurements of physical properties of the analog liquid can be found in Buliński (2004).

Physical properties of the air, including its density are assumed to be constant and equal to their values at temperature 20°C.

3.2.2 Epoxy resin. Most of physical properties of epoxy resin were assumed constant based on its data sheets obtained from the manufacturer. However, in the case of viscosity, additional measurements are required since this property is significantly influenced by the temperature and the polimerisation reaction. A polimerisation reaction is accompanied by epoxy curing and a strong exothermic effect that influences the temperature filed. Therefore, a strong coupling between the velocity and temperature fields is expected. However, measurements of polimerisation reaction kinetics with use of a DSC, reveal that the reaction starts at a temperature of about 150°C and this is significantly above the maximum experimental temperature. Therefore, this effect is neglected in the presented work.

For, the viscosity of epoxy resin, the following model is applied:

$$\mu = \mu_{\mathrm{inf}}\exp^{((U/RT)+\kappa\beta)} \tag{17}$$

where μ_{inf} stands for the initial viscosity, U is the activation energy, R is the universal gas constant, κ represents the model parameter and β is the degree of cure of the epoxy resin. Since, polimerisation reaction is neglected, the last term in the exponent of formula (17) may be dropped and this results in the formula:

$$\mu = \mu_{inf} \exp^{(U/RT)} \tag{18}$$

The parameters μ_{inf} and U of this model are found by fitting equation (18) to the measurement data (Figure 9). The epoxy resin viscosity measurements were carried out with the Brookfield LVDV-II viscometer in the temperature range from 24 to 50°C. The activation energy U is 48,046.7 J/mol and the initial viscosity μ_{inf} is equal to 2.2173×10^{-9} Pa s. The above model is implemented in the commercial CFD code Fluent through the user defined function capabilities.

In analysed problem, solution may be extremely sensitive to the values of the viscosity and its variation with temperature and curing degree. Also substantial influence of surface tension and contact angles is expected. Although these physical properties were measured, further work will cover the sensitivity analysis of mentioned parameters on the solution, especially on the free surface mapping and the temperature field in the epoxy resin.

3.3 Numerical model

Based on the dimensions of the physical model of the experimental stand in both experiments, the geometry and the numerical grid for the considered problems are created using Gambit pre-processor software. The advantage of two symmetry planes is taken into account and models are restricted only to one quarter of the casting mould.

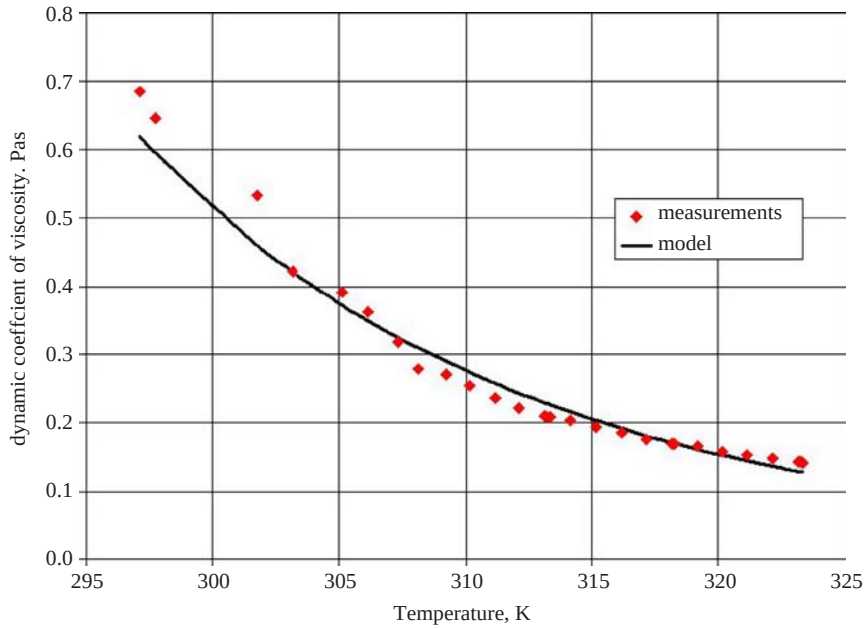

Figure 9.
Results of the epoxy resin viscosity measurements

In the case of the isothermal simulations, the geometry represents the internal volume of the mould and a piece of the feeding pipe (Figure 10). Calculations are preformed on three different grids with 145,753, 255,278 and 509,420 hexahedral cells.

For the hot experiment heat transfer in the solids which took part in the process is also considered. Therefore, the numerical model consists of the mould interior, internal transformer elements and the walls of the mould (Figure 11). For these calculations only one grid is used with 314,374 hexahedral cells. Mesh sensitivity study for this case will be carried out in further work.

In both models at all wall boundaries a zero velocity and zero normal derivative of the pressure is assumed. At the inlet to the mould a value of the velocity is prescribed.

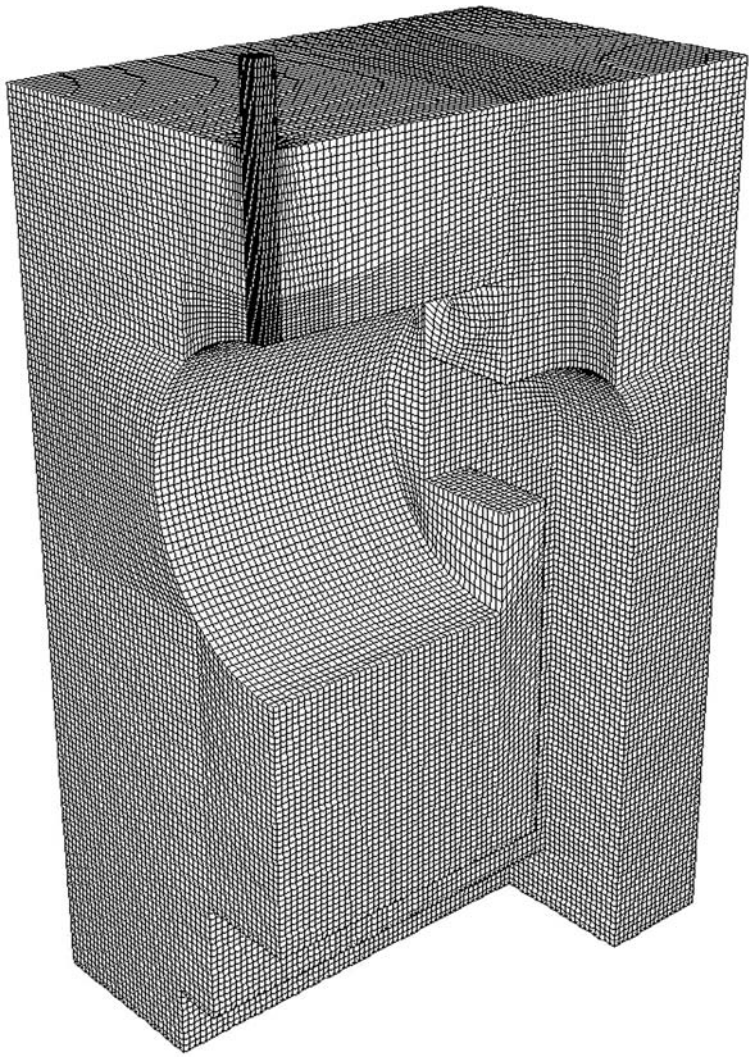

Figure 10.
Numerical grid for the isothermal transformer moulding process

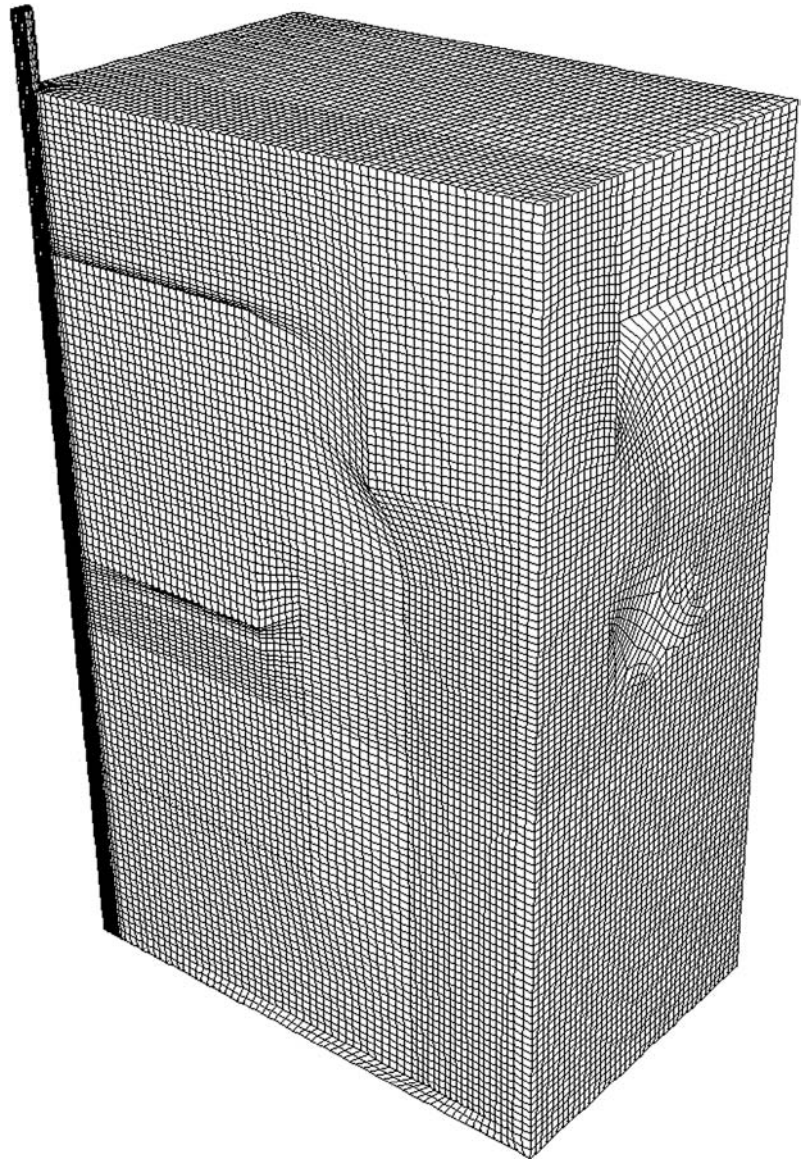

Figure 11.
Numerical grid for the non-isothermal transformer moulding process

Through the inlet only a liquid phase inflows to the computational domain. In the case of a non-isothermal model, the temperature of the inflowing liquid is prescribed. The whole mould is open to the surrounding air, and therefore the pressure is assumed on this boundary. If back flow occurs at this boundary then the temperature of inflowing air is the same as those in the surrounding air. At the symmetry planes the derivatives of all the variables in the normal direction are assumed to be zero. In the non-isothermal model at the walls attached to the solid and fluid continua

the temperature continuity condition is used. On the external walls the convective and radiative heat transfer condition is applied with a constant heat transfer coefficient and surface emissivity. The bottom of the mould is assumed to be insulated.

In both experiments, initially there is no liquid in the mould and the inlet pipe is filled with liquid and this is reflected in the initial conditions used in the mathematical model. In the non-isothermal experiment, internal elements were heated up to the temperature 393 K and placed in the mould 230 s before the casting started. Therefore, the temperature and velocity fields of the air inside the mould and the temperature of the transformer internal elements are not specified exactly at the start of the casting. To obtain the initial conditions, cooling of the internal elements inside the mould is simulated and the results are applied as initial conditions for the casting simulation (Figure 12).

4. Results and discussion

Experimental validation of the both mathematical models is mainly accomplished by comparison of the numerical results with the experimental recordings at a specified instance of time. However, it is also possible to distinguish the characteristic parameters of this flow which may provide a useful validation method. In this case, parameters such as the width of the liquid stream at the coil's top is selected. The grids plotted on the surfaces of the internal elements allow the measuring of approximate values for this parameter. Here, the intensity and the hue plots along the surface of the top coil is made and the liquid stream borders are found as abrupt changes in the intensity (Rus, 1999). Exemplary plot of the image properties (hue and intensity) for the isothermal experiment is shown in Figure 13.

In the case of the non-isothermal moulding experiment comparisons of the free surface shapes were complemented with comparison of the temperature readings from thermocouples with the temperatures calculated in the CFD model.

4.1 Isothermal moulding

For solution verification purpose, calculations for this case were provided for three meshes with different densities (see previous section). Based on these three solutions and the use of Richardson extrapolation rule (Roy, 2005), discretisation error may be estimated. Provided that, the two numerical solutions f_1 and f_2, first on coarse and the

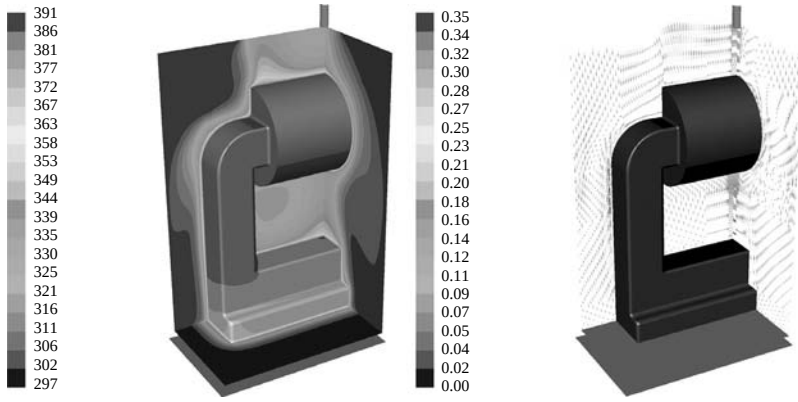

Figure 12.
Initial conditions for (a) temperature and (b) velocity fields of the air. These were obtained from the preliminary simulation

second on fine mesh are available then the extrapolated exact solution f_{exact} may be estimated:

$$f_{\text{exact}} = f_2 + \frac{f_2 - f_1}{r^p - 1} \tag{19}$$

where r stands for the mesh refinement index, which is defined here as a ratio of the mean size of the coarse grid to the mean size of fine grid, and p is the order of the accuracy of the spatial discretisation scheme. The above estimate is $p + 1$ order accurate. Since, the first-order accurate scheme is utilised for the discretisation of the governing equations hence, the estimate used in equation (19) is second-order accurate, relative discretisation error RDE may be defined as:

$$\text{RDE} = \frac{|f_{\text{exact}} - f_2|}{f_{\text{exact}}} \tag{20}$$

Equations (19) and (20) are applied to the global solution which in this case is the stream width at the top of the transformer coil. Results for the calculations at a few chosen time instances are presented in Table I. It can be seen, that for later time instances, the extrapolated solutions correspond very well with the measured values. The results obtained for earlier time instances, are not as good and this which may be the influence of the initial conditions which may not accurately reflect the experiment. Further, the Richardson extrapolation procedure is valid for smooth solutions in the asymptotic grid convergence region.

Figure 14 shows a comparison of the experiment results with the results obtained from the calculations at one specific time instance on a few different numerical grids. It can be seen that for the finest grid, the results obtained are closest to the experimental data. For the two coarser grids, at the bottom of the transformer core non physical liquid surface fluctuations appear which are not present in the experiment.

4.2 Non-isothermal moulding

As in the isothermal case, the liquid stream width obtained from the measurements is compared with that obtained from the CFD simulations (Table II). As distinct from the isothermal solution it can be noticed that here the deviation from the measurements is considerably larger and reaches almost 20 per cent. This is confirmed by comparison of the free surface mapping in the numerical model with experimental data (Figure 15). It is seen that the numerical grid is not sufficiently fine to capture appropriately the free surface, especially in regions where it undergoes large deformations.

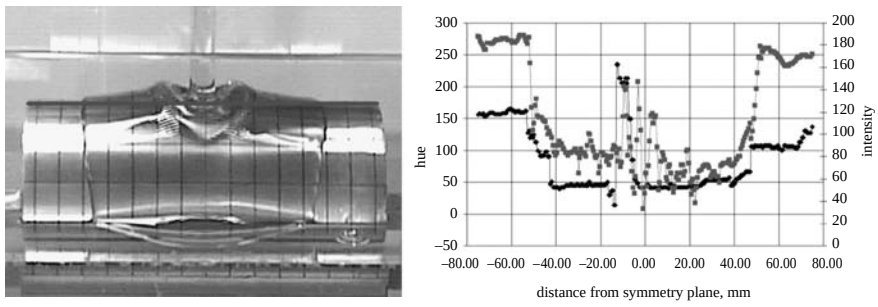

Figure 13.
Variations of the intensity and the hue along the red line at the top of transformer's coil in the isothermal experiment at time 90 s

Time (s)	First grid. 145,753 cells			Second grid. 255,278 cells			Third grid. 509,420 cells			Experiment		
	Liquid stream with (cm)	Extrapolated solution (cm)	Relative discretisation error	Liquid stream width (cm)	Extrapolated solution (cm)	Relative discretisation error	Liquid stream width (cm)	Extrapolated solution (cm)	Relative discretisation erro	Liquid stream width (cm)	Absolute error (cm)	Relative error
0.2	4.40	–	–	4.50	4.99	0.10	4.50	4.50	0.00	4.1	0.3	0.08
1.00	8.18	–	–	8.16	8.06	0.01	8.18	8.26	0.01	7.2	0.2	0.02
2.0	9.43	–	–	9.53	10.02	0.05	9.36	8.70	0.08	7.9	0.2	0.02
5.0	10.42	–	–	10.40	10.30	0.01	10.35	10.16	0.02	8.7	0.2	0.02
10.0	10.60	–	–	10.70	11.19	0.04	10.63	10.36	0.03	9.3	0.2	0.02
30.0	10.78	–	–	10.75	10.60	0.01	10.63	10.17	0.05	10.2	0.2	0.02
50.0	10.78	–	–	10.75	10.60	0.01	10.63	10.17	0.05	10.2	0.2	0.02
70.0	10.78	–	–	10.75	10.60	0.01	10.63	10.17	0.05	10.3	0.2	0.02
90.0	10.78	–	–	10.75	10.60	0.01	10.63	10.17	0.05	10.4	0.2	0.02
100.0	10.84	–	–	10.78	10.49	0.03	10.69	10.34	0.03	10.6	0.2	0.02

Table I.
Liquid stream width for the isothermal case at the surface of transformer's coil: comparison of measurements and computational results

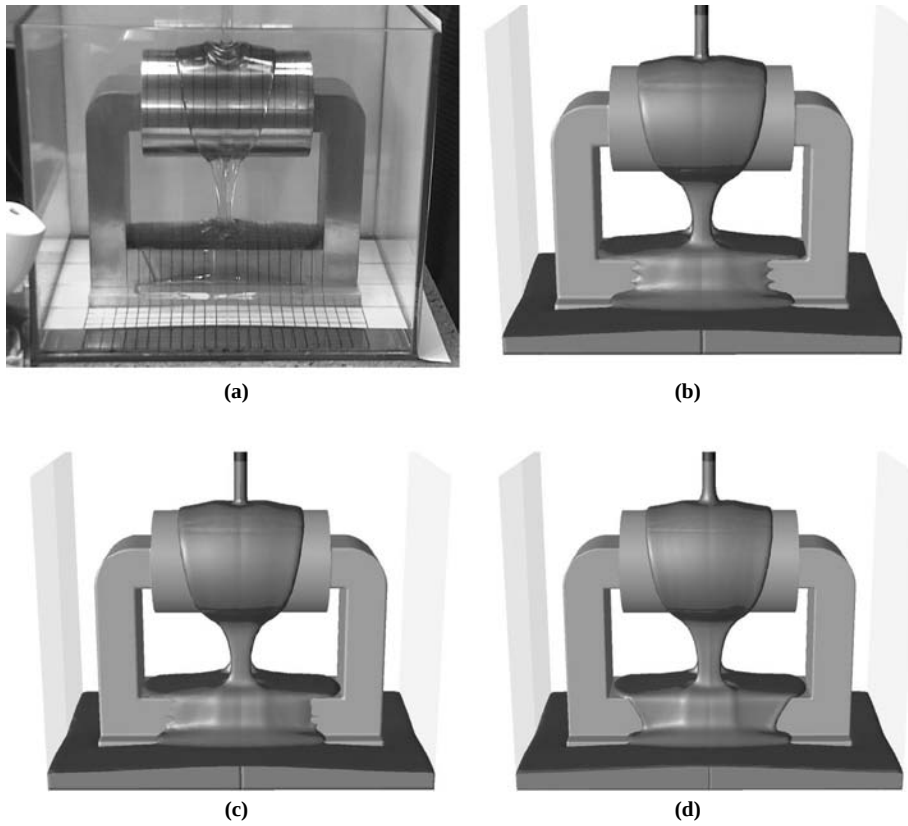

Figure 14.
Free surface after 10 s of moulding process:
(a) measurements,
(b) first grid with 145,753 hexahedral cells,
(c) second grid with 25,5278 hexahedral cells,
(d) third grid with 509,420 hexahedral cells

Table II.
Liquid stream width for the non-isothermal case at the surface of transformer's coil: comparison of measurements and computational results

Time (s)	Measurements Liquid stream width (cm)	Absolute error (cm)	Relative error	Calculations Liquid stream width (cm)
2	6.6	0.2	0.03	5.2
10	6.9	0.2	0.03	5.7
50	7	0.2	0.03	6.2
100	7.3	0.2	0.03	6.5
200	7.5	0.2	0.03	6.7
250	7.5	0.2	0.02	6.7
270	7.5	0.2	0.02	6.7

Figure 16 shows a comparison of thermocouple readings during the moulding experiment with the temperature values at the same points obtained from the CFD simulations. In both cases the same effect of a rapid increase in the temperature when the liquid surface reaches given thermocouple can be noticed. In the case of the simulations, this effect is blurred because the phase interface is smeared across a few numerical cells. That is why peak temperature is lower in the simulation and its width

is larger compared with the experimental data. This effect may be explained by the variation of the liquid density with temperature, since the density of the cold liquid is larger than the hot one, it is displaced by the latter due to buoyancy forces. This temperature stratification is very well shown in the Figure 17.

5. Summary

The presented work shows an enhanced approach to the V&V of a numerical calculations of transformer moulding process. The main objective of the presented work was to build an appropriate experimental stand and perform simple validation of the considered processes. Validation was carried out by a visual comparison of images obtained during the experiment with CFD simulations, examination of some of the characteristic parameters and through temperature measurements made inside the mould. Two cases were considered, the first was the isothermal case with an analog liquid used instead of an epoxy resin and the second one was the non-isothermal case

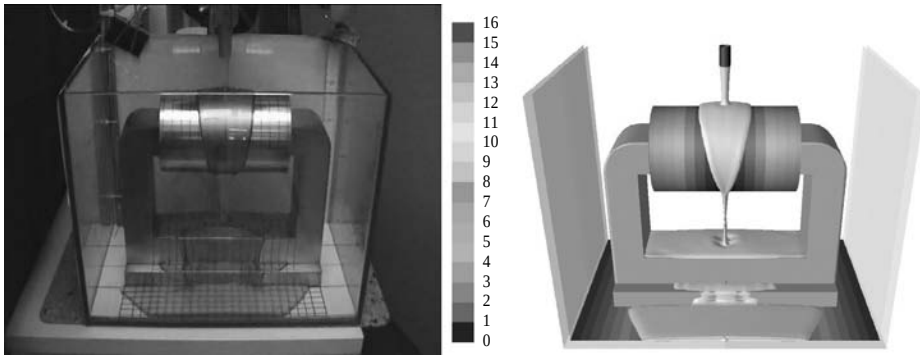

Figure 15.
Free surface after 5 s of the moulding process for the non-isothermal case: comparison between calculations and measurements

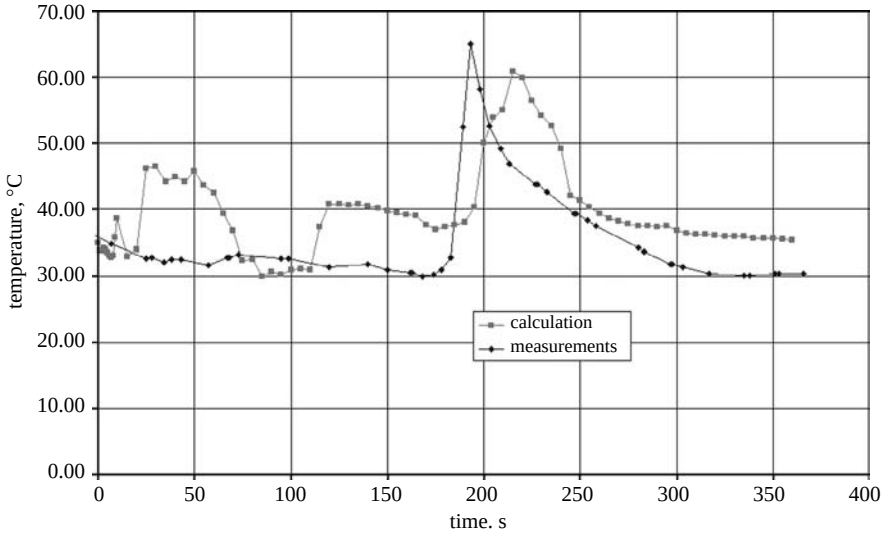

Figure 16.
Comparison of the thermocouple readings with the temperatures predicted by the CFD simulation for non-isothermal case

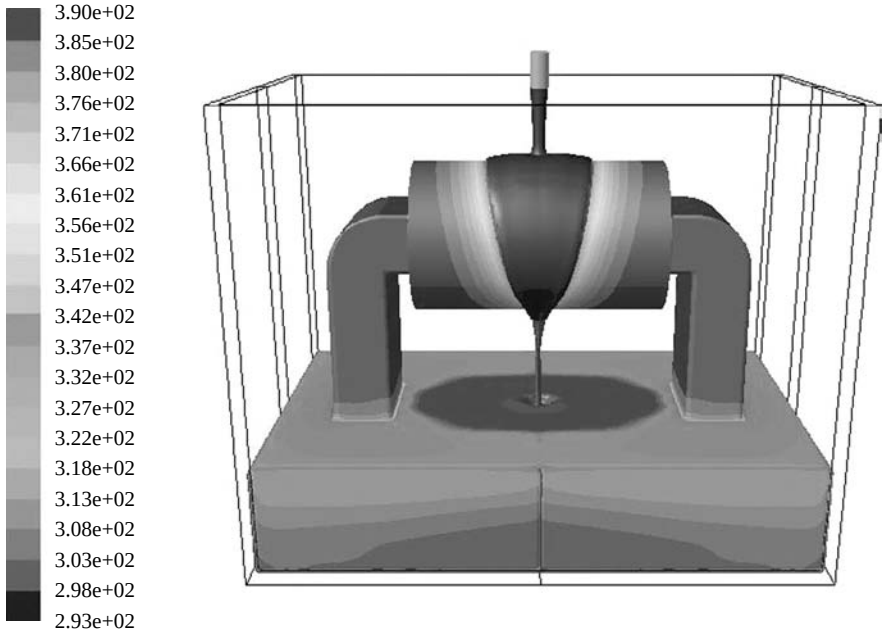

Figure 17.
Results of the calculations after 90 s for the non-isothermal case. The liquid surface and transformer's coil and core are coloured by the temperature in °K

with epoxy resin used for the moulding. For the first of analysed cases a mesh independence study and a discretisation error estimation was carried out. Simulation results show good agreement with the experimental data. Solutions found with the use of the Richardson extrapolation method corresponded very well with the measured value of width of liquid stream at the transformer's top. Although the Richardson extrapolation procedure is restricted to smooth solution which is in asymptotic grid convergence region and to grids with uniform spacing, it was successfully applied in this complex case with a nonuniform grid present and solution discontinuities.

The results obtained for the second case are not as good and discrepancy between the calculated and measured results were significant. However, still some of the effects observed during the experiment were successfully captured by the numerical simulations, e.g. the liquid stratification. The main problem in the simulations of this problem appears to be that there is not sufficient accurate information about the physical properties of the epoxy resin and their variations with temperature, especially its surface properties such as surface tension and contact angle.

In general, CFD simulations of electrical transformer moulding processes with the use of the VOF model revealed good agreement with experimental data. Characteristic elements of the liquid free surface shape were satisfactory mapped. This is promising for further utilisation of the VOF model in simulations of such processes.

References

Babuska, I. and Oden, I.T. (2004), "Verification and validation in computational engineering and science: basic concepts", *Computer Methods in Applied Mechanics and Engineering*, Vol. 193 Nos 36/38, pp. 4057-66.

Banaszek, J. (2005), "Credibility analysis of computer simulation of complex heat transfer problems", in Nowak, A.J., Białecki, R. and Węcel, G. (Eds) *Eurotherm Seminar 82 Numerical Heat Transfer 2005 Conference*, 13-16 September, Gliwice-Cracow, Silesian University of Technology Publishing House, Gliwice, pp. 141-63.

Brackbill, J.U., Kothe, D.B. and Zemach, C. (1992), "A continuum method for modelling surface tension", *Journal of Computational Physics*, Vol. 100 No. 2, pp. 335-54.

Buliński, Z. (2004), "Numerical analysis and experimental verification of fluid flows with free boundary in electrical transformers moulding processes", MSc thesis, Silesian University of Technology, Gliwice.

Harlow, F.H. and Welsh, J.E. (1965), "Numerical calculation of time dependent viscous incommpressible flow with free surface", *Physics and Fluids*, Vol. 8, pp. 2182-9.

Hirt, C.W. and Nichols, B.D. (1981), "Volume of fluid (VOF) method for the dynamics of free boundaries", *Journal of Computational Physics*, Vol. 201, p. 225.

Mingming, T. and Browne, D.J. (2005), "Modelling of gas atomisation of melt flow", in Nowak, A.J., Białecki, R. and Węcel, G. (Eds) *Eurotherm Seminar 82 Numerical Heat Transfer 2005 Conference*, 13-16 September, Gliwice-Cracow, Silesian University of Technology Publishing House, Gliwice, pp. 387-96.

Roy, Ch.J. (2005), "Review of code and solution verification procedures for computational simulation", *Journal of Computational Physics*, Vol. 131, p. 156.

Rus, J.C. (1999), *The Image Processing Handbook*, CRC Press, Boca Raton, FL.

Sekuła, R., Kaczmarek, K., Saj, P., Forsman, K., Mahonen, P. and Leskosek, H. (2002), "Reactive molding: from simulation to reality", *ABB Review: The Corporate Technical Journal of the ABB Group*, No. 1, pp. 64-7.

Tryggvason, G., Bunner, B., Esmaeeli, A., Juric, D., Al-Rawahi, N., Tauber, W., Han, J., Nas, S. and Jan, Y.J. (2001), "A front-tracking method for the computations of multiphase flow", *Journal of Computational Physics*, Vol. 169 No. 2, pp. 708-59.

Further reading

ABB Group (2001), "Power IT voltage transformer indoor, UMZ", *Catalogue*, ABB Group, Zurich.

ABB Group (2004), *Instrument Transformer, Technical Information*, ABB Group, Zurich.

Buliński, Z., Nowak, A.J. and Saj, P. (2005), "Numerical analysis and experimental validation of the free surface flow and heat transfer in electrical transformers moulding processes", in Nowak, A.J., Białecki, R. and Węcel, G. (Eds) *Eurotherm Seminar 82 Numerical Heat Transfer 2005 Conference*, 13-16 September, Gliwice-Cracow, Silesian University of Technology Publishing House, Gliwice, pp. 1025-35.

Czub, P., Bończa-Tomaszewski, Z. and Penczek, P. (2002), *Chemistry and Technology of Epoxy Resins*, WNT, Warsaw (in Polish).

Ferziger, J.H. and Perić, M. (1999), *Computational Methods for Fluid Dynamics*, Springer, Berlin.

Scardovelli, R. and Zaleski, S. (1999), "Direct numerical simulation of free-surface and interfacial flow", *Annual Reviews of Fluid Mechanics*, No. 31, pp. 567-603.

Corresponding author

Zbigniew Buliński can be contacted at: zbigniew.bulinski@polsl.pl; bulinski@itc.polsl.pl